Fourier transform infrared (FTIR) instrumentation for monitoring recovery boilers

Philip W. Morrison Jr., Joseph E. Cosgrove, Robert M. Carangelo, Martin D. Carangelo, and Peter R. Solomon, Pierre Leroueil, and Peter A. Thorn

In Longview, FTIR acts as an on-line diagnostic tool for Weyerhaeuser's recovery boiler. So far, the concentrations of various gases and fume particles have been successfully analyzed.

One of the key unit operations in the kraft pulping process is the firing of the recovery boiler. The primary purpose of the recovery boiler is to reclaim the sodium and sulfur contained in the black liquor by-product of the pulping process. The boiler's secondary function is to burn the lignin found in the liquor to generate energy. The recovery boiler accomplishes these twin goals by burning concentrated black liquor in a large furnace (about 10 m across).

The combustion process produces both a liquid smelt of Na_2CO_3 and Na_2S on the floor of the boiler and an aerosol fume composed of primarily Na_2SO_4 and Na_2CO_3. Both of these products contain Na and S to be recovered. The liquid smelt simply pours off the boiler bed and falls into dissolving tanks for recovery. Recovering the fume is much more difficult because one must separate the fume particles from the combustion gases and recycle the fume with the feedstock of black liquor. This task usually requires an electrostatic precipitator and other dust-handling equipment.

Efficient operation of the recovery boiler depends on balancing chemical recovery efficiency and energy efficiency. On one hand, operators want to minimize the amount of sulfur lost through the stack as gaseous compounds (H_2S, mercaptans, and SO_x) and as fume. The reasons are both economic and environmental. Fortunately, the fume formation process seems to help control these problems (*1*). On the other hand, high fuming rates burden the precipitator and coat the heat exchanger surfaces with deposits. Removing these deposits with high-pressure steam (sootblowing) represents a substantial energy cost. In addition, the operators want to maintain high energy efficiency (which means a low CO concentration). Achieving a balance among all these factors is an optimization arrived at empirically on the basis of decades of operating experience.

Future improvements in boiler design and operating efficiency are limited by two main factors. First, there is little understanding of the detailed physics and chemistry of the recovery process. Second, there have been no sophisticated sensors that can function in the demanding environment of the boiler. Because there is no model for understanding the process chemistry, one cannot operate the boiler at its peak efficiency nor design improved boilers. Developing such models is slow because laboratory-scale experiments are not realistic and because scientists lack sensors that can provide useful information on the gas and particle properties inside the boiler. Under the best circumstances, a well-equipped recovery boiler may have thermocouples, infrared bed cameras, opacity meters, and chemical sensors for O_2, CO, and total reduced sulfur. These are inadequate for the task of elucidating the boiler chemistry. Even if one understood the chemistry, the boiler operators would still need rugged, sophisticated sensors to provide feedback for an improved process control loop.

Here, we describe a new technique to contend with the sensor and diagnostic problems in the recovery boiler. The technique uses Fourier transform infrared (FTIR) spectroscopy and relies on a combination of emission and transmission measurements (E/T). By interpreting E/T FTIR measurements, one can determine gas properties like concentration and temperature and also particle properties like number density, size, and temperature. The technique has been tested in the laboratory on various

Morrison is manager, Process Monitering Group, Cosgrove is research assistant, R. Carangelo is manager, FT-IR Products, M. Carangelo is research assistant, and Solomon is president with Advanced Fuel Research, Inc., 87 Church St., East Hartford, CT 06108. Leroueil is research engineer and Thorn is senior process engineer at Weyerhaeuser Paper Co., Tocoma, WA 98477.

1. The long-throw optics apparatus consists of a beam expander on the spectrometer (left) and a beam condenser on the transmission detector and housing (right).

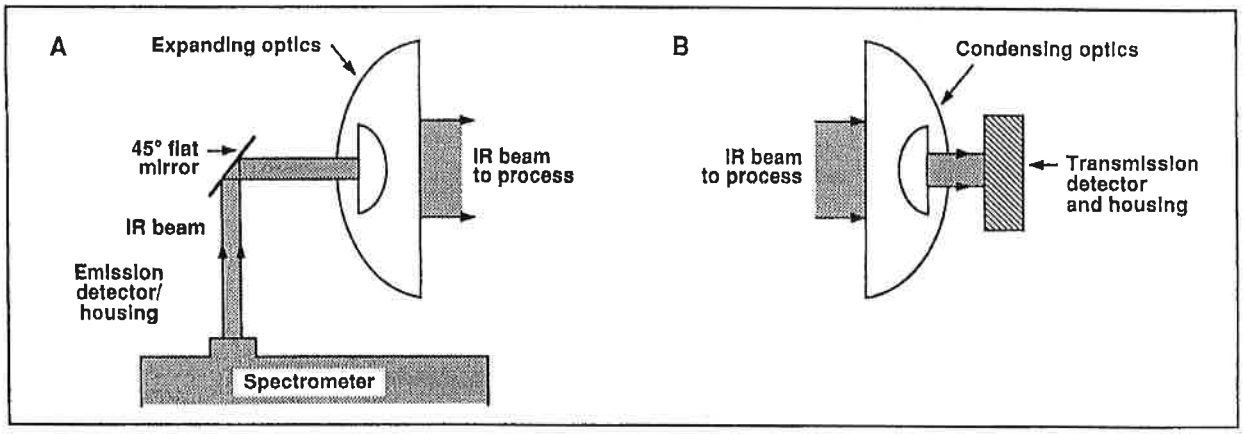

2. The FTIR spectrometer is coupled to the recovery boiler. Points A and B show the configuration for acquiring the *ex-situ* reference.

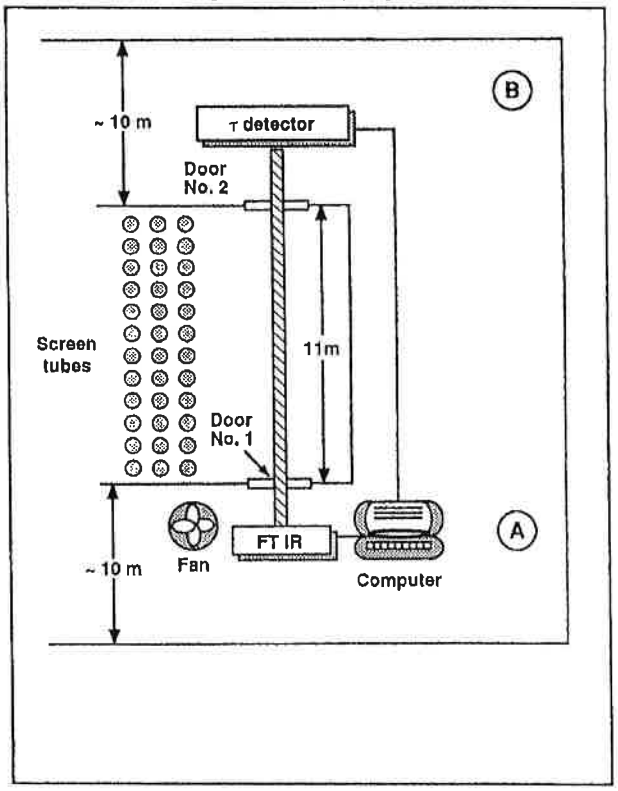

combustion systems (*2–4*), including coal flames. Advanced tomographic techniques can deconvolute E/T spectra to yield point values for the gas and particle properties in small flames (*5, 6*).

In this work, we have applied the E/T FTIR method to a large recovery boiler located at the Weyerhaeuser mill in Longview, WA. These tests show that the E/T FTIR spectrometer can obtain line-of-sight averages for species concentrations and temperature measurements across an 11-m-wide boiler.

Apparatus

FTIR system

The FTIR apparatus consists of a spectrometer, a set of long-throw optics to project the IR beam through the boiler, two detectors to acquire emission and transmission spectra, and a computer to operate the spectrometer and analyze the data. The spectrometer is a Bomem M110 spectrometer modified in our laboratory to acquire emission and transmission scans concurrently with no change in the optical path. The M110 design is a corner cube interferometer that can accept two different sources and detectors. In the modified design, one source is the globar (transmission), and the other is the process stream (emission). A "scan" by the spectrometer consists of a forward and reverse motion by the moving mirror. During the forward motion, the transmission detector sends its signal to the computer; the emission detector sends its signal to the computer during the reverse motion. To average signals, the computer coadds each half scan separately. The M110 has a fixed resolution of 4 cm^{-1} and scans the spectral region between 6500 and 500 cm^{-1} (1.5–20 μm).

The long-throw optics apparatus, depicted in **Fig. 1**, consists of a beam expander on the spectrometer and a beam condenser on the transmission detector. Expanding the beam helps keep the infrared beam collimated over long distances by reducing beam divergence. To maximize the signal-to-noise ratio, the spectrometer has HgCdTe detectors that require liquid nitrogen cooling. In the future, we expect to make measurements using less sensitive pyroelectric detectors that operate at ambient temperature. To simplify and automate the data acquisition process, we use a computer running software purchased from Spectra Calc (Galactic Industries) and modified in this laboratory.

The FTIR measurements take place 36.5 m (120 ft) above the smelt bed, near the screen tubes (**Fig. 2**). The boiler is about 11 m wide (36 ft) and has two doors that lie across from one another. The door openings are 5 cm × 20 cm. At this level, the process stream is a complex mixture of combustion by-products like N_2, O_2, CO_2, H_2O, other trace gases, and fume particles. The boiler is at a slight negative

$$R_n(\nu) = R(\nu)/[1 - \tau(\nu)] = \frac{k_i(\nu)C_i R_b(\nu, T_{gas}) + NAF_{abs}(\nu)R_b(\nu, T_p) + NAF_{scn}(\nu)R_b(\nu, T_{wall})}{k_i(\nu)C_i + NAF_{ext}(\nu)} \quad (2)$$

$$Q_{ext} = 4x \text{ Imag}\left\{z(m)\left[1 + \frac{x^2}{15} z(m)\left(\frac{m^4 + 27m^2 + 38}{2m^2 + 3}\right)\right]\right\} + \frac{8}{3}x^4 \text{ Real}\left\{z^2(m)\right\} \quad (4)$$

pressure (approximately 1 in. of water), so windows are not required.

Turbulence in the boiler, however, causes puffs of fume to exit from the doors, and the puffs extend about 2 m from the wall of the boiler. To minimize fume contamination on the beam expander, the spectrometer is located about 3 m from Door 1, and a fan blows the fume away from the spectrometer (Fig. 2). On the other side of the boiler, the transmission detector is located about 6–7 m from Door 2. This position keeps fume away from the optics and minimizes vibration from the floor. (The current design of the alignment system for the transmission detector has no provision to reduce vibration.) Together, these constraints yield a total pathlength from spectrometer to detector of 21 m (70 ft). Using this configuration, vibration does not significantly detune the optics over the course of three days.

The FTIR measurements use two distinct optical configurations. All boiler measurements use the configuration shown in Fig. 2. The alignment of the IR beam through the two doors is done "blind" because the fume particles scatter all visible light crossing the boiler. The second optical configuration is necessary so that one can acquire a reference spectrum for the transmittance measurements: $\tau(\nu) \equiv$ sample spectrum/reference spectrum, where ν = wavenumber, in cm^{-1}. Under laboratory conditions, one would normally remove the sample and acquire the reference. In the recovery boiler, however, removing the sample requires shutting down the boiler, so it is not possible to acquire the reference spectrum under most circumstances.

For this feasibility test of the FTIR, we have adopted a less desirable but reasonably effective alternative for acquiring the reference spectrum. Instead of acquiring the reference through an empty boiler (*in-situ* reference), one can acquire a reference scan outside the boiler (*ex-situ* reference) and can assume that the *in-situ* reference and *ex-situ* reference are roughly the same. This assumption is a good one if the beam expander has an aperture that limits the beam size and if the distance between the spectrometer and detector is the same. Points A and B in Fig. 2 show the configuration for acquiring the *ex-situ* reference.

The data presented here show the configuration for acquiring the *ex-situ* reference. For these data, an *ex-situ* reference was actually averaged from three different conditions. Two of the references were acquired using the same position but were taken one day apart. The third reference was taken after moving the detector 1 m to the side. None of the three individual references varies by more than 5% from the average as long as $\nu < 5000\ cm^{-1}$; the variation is 10% for $\nu > 5000\ cm^{-1}$. Future experiments comparing *in-situ* references and *ex-situ* references will determine the accuracy of the above assumption.

I. Operating conditions of Recovery Boiler No. 10

	Low flow	*High flow*
Black liquor		
Flow, gal/min	200	325
Solids content, %	67	67.5
Temperature, °F	237	233
Pressure, psig	29.4	31.4
Air flow, 1000 lb/h		
Primary	273	296
Secondary	282	330
Tertiary	152	162
Steam flow, 1000 lb/h	350	550

Recovery boiler

Longview's Boiler No. 10 is a Babcock and Wilcox design using four liquor guns. It has a three-level air system and a rated capacity of 3.6 million pounds of black liquor solids per day. During the five days of FTIR measurements, the boiler operators used the two different firing conditions described in **Table I.**

Data analysis

Emission/transmission analysis

The analysis of the E/T data follows the procedures outlined in Best *et al.* (2). The transmittance spectra yield concentration information for the gases and particles. The combined analysis of radiance (emission) and transmittance spectra determines gas and particle temperatures. Here, we will briefly outline the procedures.

The transmittance is related to concentration via Eq. 1:

$$\tau(\nu) = \exp\left[-\left[k_i(\nu)C_i + N\,A\,F_{ext}(\nu)\right]L\right] \quad (1)$$

where

$\tau(\nu)$ = transmittance

$k_i(\nu)$ = absorptivity for the gas i, cm^2/mole

C_i = concentration of the gas i, mol/cm^3

N = number density of particles, no./cm^3

A = projected area of a particle, cm^2

$F_{ext}(\nu)$ = extinction efficiency for a particle (dimensionless)

L = path length of the infrared beam through the sample, cm

The first term arises due to gas absorption, and the second term is the result of particle absorption and scattering. The parameters $k_i(\nu)$ and $F_{ext}(\nu)$ are usually independent of C_i and N, respectively, except when C_i and N are very large. The major difference between the two is that gas absorption bands sharply peak in spectral regions a few hundred wavenumbers wide, whereas $F_{ext}(\nu)$ is a quantity that varies smoothly across the whole spectrum.

The combination of the gases and particles produces a spectrum with gas absorption peaks superimposed upon a baseline shift caused by particle extinction. Simple baseline subtraction can easily isolate the two effects. Furthermore, Mie theory (*7*) can be used to predict the form of $F_{ext}(\nu)$, given the particle size, particle optical constants, and acceptance angle of the spectrometer. In Eq. 1, it is assumed that there is only one kind of particle and only one size. One can extend the analysis to include multiple particles and sizes by replacing $N\ A\ F_{ext}$ with the sum: $\Sigma\ N_j A_j F_{ext,j}(\nu)$.

A quantity called the "normalized radiance," $R_n(\nu)$, yields temperature information and is defined as the ratio $R(\nu)/[1-\tau(\nu)]$ where $R(\nu)$ = sample radiance. As in the case of the transmittance spectrum, one must correct the as-measured radiance for instrumental artifacts using an instrument response function (path correction). The most convenient method is to place a black body standard of known spectral radiance and measure the instrument response function. After such a correction, the radiance relates to gas and particle temperatures as described in Eq. 2.

See Eq. 2.

where

$R_b(\nu,T)$ = the Planck spectral function for a black body at temperature T

T_{gas} = gas temperature

$T_{particle}$ = particle temperature

T_{wall} = wall temperature

$F_{abs}(\nu)$ = absorption efficiency of a particle

$F_{sca}(\nu)$ = scattering efficiency of a particle.

Note that $F_{ext} = F_{abs} + F_{sca}$.

Equation 2 is most easily understood and analyzed by looking at limiting cases. For example, when the gas stream contains no particles ($N = 0$), Eq. 2 predicts that the normalized radiance is identical to $R_b(\nu,T_{gas})$ wherever k_i is nonzero. In the case in which the sample contains both particles and gases, one can use the baseline to correct the transmittance and radiance to remove the particle contributions. Calculating the normalized radiance from the corrected spectra yields the gas temperature as if it were the no-particle limiting case.

One can perform slightly different manipulations of Eq. 2 to yield the particle and wall temperatures. In the spectral regions where the particle absorption is very strong, then $F_{ext}(\nu) \sim F_{abs}(\nu)$. If gas absorptions are also small (where $k_i(\nu) = 0$), Eq. 2 predicts $R_n(\nu) = R_b(\nu,T_{wall})$. Similarly, at high wavenumbers ($\nu > 4000\ cm^{-1}$), one finds that both particles and gases are nonabsorbing, so that $F_{ext}(\nu) \sim F_{sca}(\nu)$, $k_i(\nu) = 0$, and $R_n(\nu) = R_b(\nu,T_{wall})$. In Eq. 2, it is assumed that the walls of the reactor behave like a black body (emissivity = 1), but this is an accurate approximation for a process stream that is almost completely surrounded by the hot walls. In this case, the intrinsic emissivity of the wall material is irrelevant, and the reactor behaves like a black body.

In both Eqs. 1 and 2, it is assumed that the properties are uniform for the gas, particle, and wall. In real systems, this uniformity is not the case, and the measured transmittance and radiance are averages along the IR beam. For the purposes of this research, this approximation is acceptable. In principle, however, one can perform a series of E/T FTIR measurements across the process stream and then tomographically reconstruct the data to produce point values for transmittance and radiance (*5, 6*). With such reconstructed data, Eqs. 1 and 2 will yield accurate concentrations and temperatures as functions of position.

Mie Theory analysis

Much of the work described here depends on predicting the extinction properties of the fume particles. Given the optical properties of the fume and the acceptance angle of the spectrometer, one can calculate F_{ext}, F_{abs}, and F_{sca} (*7*). In the case of the fume, however, several simplifications to the full Mie theory are possible.

One of the key dimensionless parameters in Mie theory is the size parameter x:

$$x = \pi D/\lambda = \pi D\nu \tag{3}$$

where

D = particle diameter

λ = wavelength of light.

For fume particles and IR radiation, x is small because fume is submicron in size and the wavelengths are 1.5–20 μm (6500–500 cm^{-1}). Under such conditions, Rayleigh extinction occurs, and the size and shape of the particle and the acceptance angle of the spectrometer are relatively unimportant. Thus, one can avoid a lengthy calculation for F_{ext}, F_{abs}, and F_{sca} and substitute the efficiencies for 0° acceptance angle. These quantities are called Q_{ext}, Q_{abs}, and Q_{sca} and are given by Eqs. 4–6 (*7*):

See Eq. 4.

$$Q_{sca} = (8/3)\ x^4\ |z(m)|^2 \tag{5}$$

$$Q_{sca} = Q_{ext} - Q_{abs} \tag{6}$$

where

x = $\pi D\nu$

D = particle diameter

m = the complex index of refraction

= $n(\nu) + ik(\nu)$

3. Optical constants of Longview fume. A: KBr pellet spectrum of fume. B: Refractive index $n(\nu)$ determined from A and using a limiting value of 1.5. C: Extinction coefficient $k(\nu)$ determined from A.

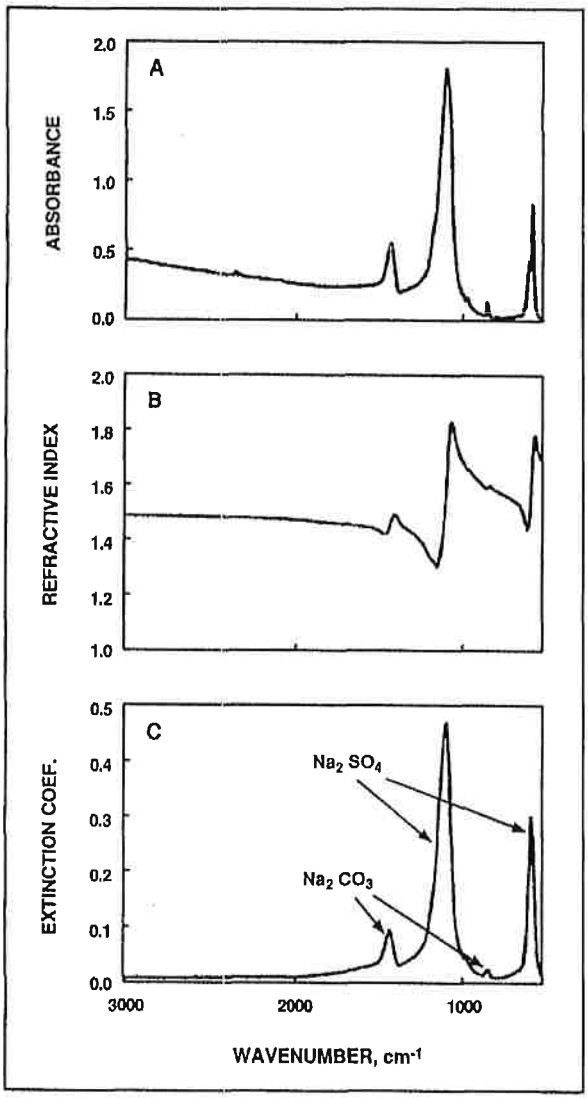

4. Representative E/T spectra. A: Transmittance through the boiler. B: Radiance from the boiler. C: Normalized radiance, with curves of two Planck functions for the gas and fume temperature (1125 K) and the wall temperature (975 K).

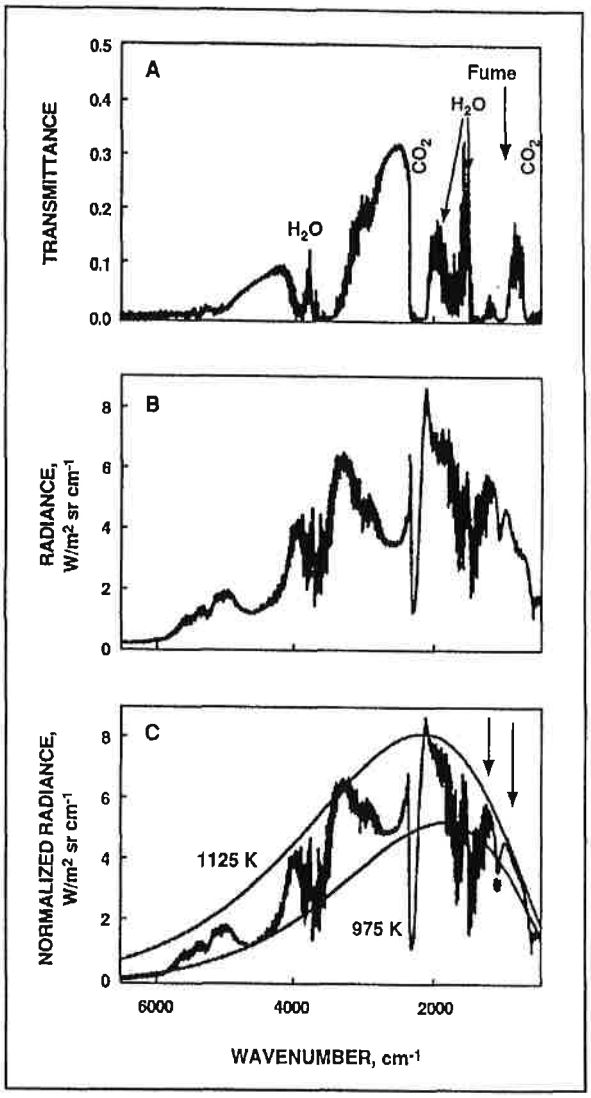

$n(\nu)$ = index of refraction

$k(\nu)$ = extinction coefficient

$z(m)$ = $\frac{m^2-1}{m^2+2}$

The symbols Imag and Real in Eq. 4 signify the imaginary or real part of the complex expression.

To calculate Q from Eqs. 4-6, one requires the optical constants for fume. We have determined $n(\nu)$ and $k(\nu)$ using the method of Solomon *et al.* (*8*, *9*). The method requires suspending the fume in pellets of KBr and CsI and measuring the IR transmittance of the pellet. Such a pellet spectrum of fume in KBr appears in **Fig. 3A**. The absorption features in Fig. 3A correspond exactly to the absorption features appearing in pellet spectra of pure Na_2SO_4 and Na_2CO_3. The relative sizes of the sulfate and carbonate peaks are consistent with the chemical analysis provided by Weyerhaeuser: approximately 45% sulfate, 13% carbonate, 3% chloride, 30% sodium, and 4-5% potassium. The K and Cl components are not observed because KCl is IR transparent and the K_2SO_4 and K_2CO_3 absorptions overlap their sodium counterparts.

By guessing a value for the average particle size and by ignoring scattering effects due to $n(\nu)$, we can use Mie theory to predict $k(\nu)$ from the measured KBr pellet spectrum. To ensure self-consistency, one then predicts the values of $n(\nu)$ corresponding to the $k(\nu)$ values using the Kramers-Kronig transform and an educated guess for the limiting value for $n(\nu)$ at high wavenumbers (n_∞).

Typically, one lets n_∞ equal the value of $n(\nu)$ in the visible. We then use these values of $n(\nu)$ and $k(\nu)$ as inputs for another Mie theory calculation that predicts the pellet

spectrum for fume in CsI. Comparing the predicted results to the actual measurements and iterating yields reasonably accurate values for the true optical constants for fume.

The results of such a calculation appear in Fig. 3B and C using the parameters n_∞ = 1.50 and particle radius = 0.35 μm. We let n_∞ = 1.50 because it is intermediate between the index of Na_2SO_4 (n = 1.480) and Na_2CO_3 (n = 1.535). Note that k(ν) accurately reproduces the absorption bands found in the pellet spectra. The calculated values for $n(\nu)$ predict a weak Christiansen effect near 1200 cm^{-1} where n = 1.31. Because particle scattering decreases sharply as the difference $n_{fume} - n_{air}$ decreases, we expect that at 1200 cm^{-1} the particles are nearly perfect absorbers ($Q_{ext} \sim Q_{abs}$), and radiance measurements should yield accurate measurements of fume temperature.

Furthermore, the calculations show that above 1600 cm^{-1}, $n(\nu)$ is very constant, and k(ν) is very low. Because of this, the particle extinction will be a minimum near 1600–1700 cm^{-1} because scattering is proportional to ν^4 (Eq. 5). Thus, the fume cloud should be completely opaque at visible and near-IR wavelengths and should be quite transparent near 1600 cm^{-1}. Using similar reasoning, fume should have another region, though not so transparent, at 750–900 cm^{-1}. Unfortunately these "windows" are obscured by H_2O absorptions, and the most transparent region is near 2500 cm^{-1}.

Results

Representative E/T spectra appear in **Fig. 4**. Although the eye cannot see through the fume because of scattering in the visible spectrum, Fig. 4A shows that the stream is quite transparent in the IR spectrum. Most of the opaque notches in the spectrum (where $\tau(\nu)$ = 0) are due to absorptions by the major gas species: CO_2 (2400–2150 cm^{-1} and 800–500 cm^{-1}) and H_2O (4100–3100 cm^{-1}, 2000–1300 cm^{-1}, and < 700 cm^{-1}).

Please note that the noise level in this spectrum is equivalent to τ_{noise} = 0.005 at 2000 cm^{-1}. The seemingly large noise level below 2000 cm^{-1} is actually discrete absorption lines of water. Since parts of the H_2O and CO_2 absorption bands are saturated, one must determine the amount of CO_2 and H_2O by analyzing the weaker edges of the absorption bands. Although the long pathlength causes the opaque parts of the spectrum to be unusable, many other gas spectra would still be detectable. For example, the absence of detectable absorption near 2883 cm^{-1} indicates that there is little HCl in the boiler (<40 ppm at a temperature of 1100 K). (In the discussion section, we will elaborate on trace gas analysis.)

Between the CO_2 and H_2O bands, the extinction properties of the fume manifest their effects. At high wavenumbers, $\tau(\nu)$ is near 0 because the fume is highly scattering and no IR can penetrate through the 11-m fume cloud. For submicron particles, however, the scattering decreases rapidly with decreasing wavenumber, and partially transparent windows appear in the spectrum between the CO_2 and H_2O absorption bands. The region between 2500 cm^{-1} and 3000 cm^{-1} is partially transparent. The fume absorbs strongly in the region near 1115 and 615 cm^{-1}, and the spectrum is completely opaque in those regions.

Qualitatively, the radiance spectrum (Fig. 4B) is the inverse of the transmittance spectrum: wherever the transmittance is high, the radiance is low. Strong absorption regions of both gases and particles emit strongly since the gas and particles are hot. The CO_2 band, however, is a notable exception to this general trend. The sharp notch in the radiance near 2400 cm^{-1} results from cold CO_2 outside the boiler absorbing the radiation from the hot CO_2. At both edges of the band, however, the radiation from hot CO_2 is not absorbed by the cold CO_2, and these regions can be used to determine the hot CO_2 temperature. The highest radiance values occur in the gas bands, while the broadband radiance is lower. This observation indicates that the gas temperature is higher than the wall temperature. The radiance in the fume's absorption bands (the notch in the spectrum near 1200 cm^{-1}) shows a range of values, indicating a variety of fume temperatures.

The normalized radiance shown in Fig. 4C provides a quantitative measure of the temperatures in the boiler. The Planck curve corresponding to 1125 K fits R_n with the absorption bands of CO_2 (2200 cm^{-1} and H_2O (3500 cm^{-1}), indicating the average T_{gas} is 1125 K. A direct fit of R_b (ν, T_{gas}) to R_n without baseline correction is possible because the CO_2 and H_2O absorption bands are saturated and $k_i(\nu)C_i >> N\,A\,F_{ext}(\nu)$ (Eq. 2). Note that the notch in the CO_2 band indicates a very low temperature for the gas outside the boiler (about 700 K).

The second Planck curve corresponds to T_{wall} = 975 K since it matches the normalized radiance at high wavenumbers where the fume strongly scatters wall radiation. Interestingly, a different Planck curve (1000 K, not shown in the Fig. 4) fits R_n in the region near 2500 cm^{-1}. Since any radiance in this region is also due to scattered wall radiation (since the fume is nonabsorbing at 2500 cm^{-1}), there appears to be a second wall temperature. The lower temperature occurs in the highest scattering region ($F_{scn} \propto \nu^4$), producing an average temperature of 975 K for the wall surfaces closest to Door No. 1. On the other hand, the scattering by the fume at 2500 cm^{-1} is lower, and thus the fume scatters radiation from the walls throughout the boiler (including hotter upstream walls). As a result, the average wall temperature is 1000 K.

Similar effects occur for the fume temperature measurements. Using predictions of F_{ext} for the fume and comparing F_{ext} to the normalized radiance, one finds that the peak in F_{ext} nearly coincides with the lowest point in the notch in R_n (the asterisk near 1200 cm^{-1} in Fig. 4C). In fact, the extinction is so high at this peak that only the cooler fume contained in the outer 2–3 m can radiate to the spectrometer; hotter fume inside the boiler is completely blocked. As a result, the measured (average) temperature of this outer layer is 925 K.

In spectral regions away from the peak, F_{ext} decreases sharply, and the emission detector can "see" farther into the boiler and sample the hotter fume. As shown in Fig. 4C, the normalized radiance increases as one moves away from the asterisk. At the very edges of the fume's absorption band (arrows), the measured (average) temperature is identical to the average gas temperature: 1125 K. This experimental result agrees with the intuitive expectation that the fume and gas temperature should be the same.

5. Transmittance and normalized radiance spectra of the recovery boiler at two different flows of black liquor. In the normalized radiance, spectra also contain best-fit Planck functions for the gas and fume temperatures (upper curves) and the wall temperature (lower curves).

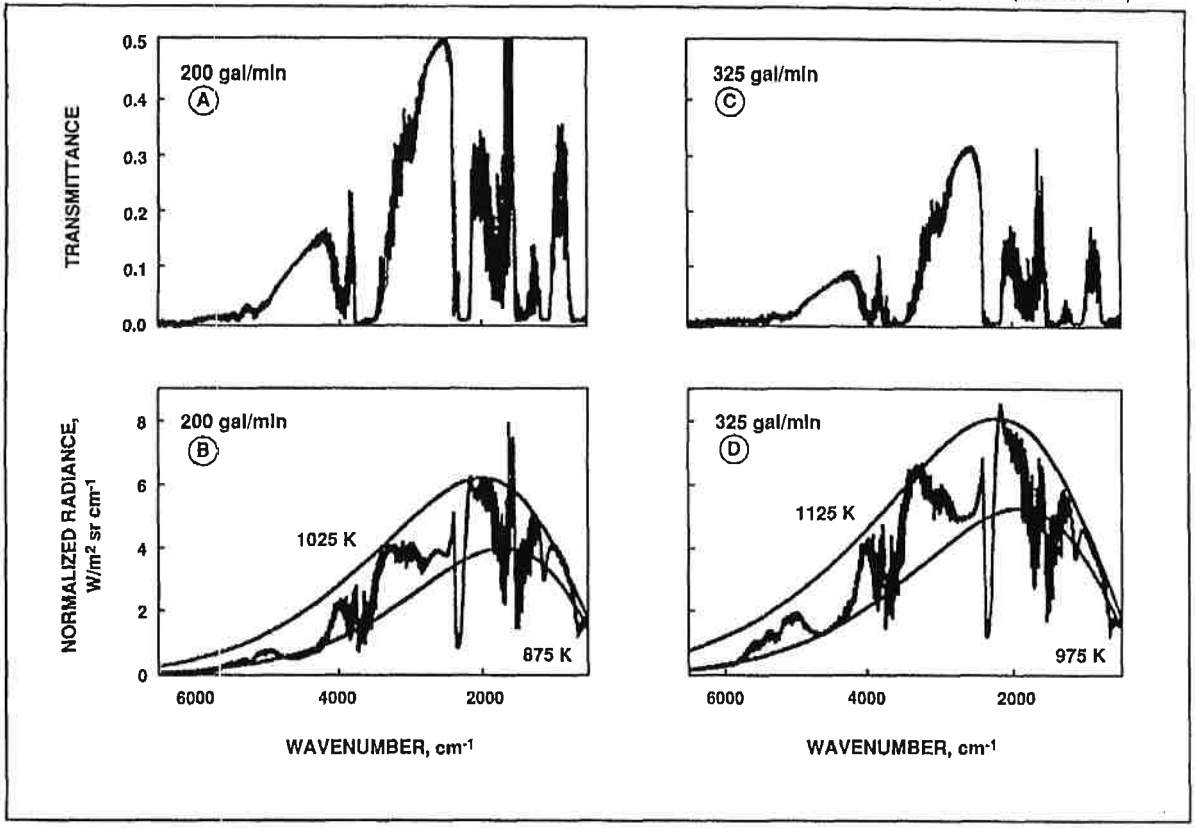

II. Sensitivity levels for various gases

	Ex-situ, 1 cm⁻¹	*Boiler, 1 cm⁻¹*	*Boiler, 4 cm⁻¹*	*Boiler + H_2O, 4 cm⁻¹*	*Boiler + H_2O + fume, 4 cm⁻¹*
		Signal averaging duration and noise level			
Time, min	16	1	1	1	1
Noise, %	0.1	0.5	0.5	0.5	0.5
		Sensitivity levels, ppm			
H_2S	256	1282	5128	5128	5128
SO_2	0.310	1.55	1.55	6.2	Blocked
$(CH_3)_2S$	1.010	5.07	5.07	5.07	5.07
CO	0.550	2.73	10.9	10.9	10.9
CS_2	0.050	0.25	0.25	Blocked	Blocked
COS	0.063	0.31	0.31	0.31	0.94
NO	1.000	5.00	20.0	...	286
NO_2	0.230	1.16	1.16	...	5.60
NH_3	0.160	0.80	3.2	3.2	3.20
HCl	0.510	2.54	10.2	10.2	10.2

Assumptions: Standard temperature and pressure. Absorption = 3 times the noise level. Pathlength = 11 m. HgCdTe detectors.

6. Transmittance spectra of the recovery boiler with a nearby sootblower off and on

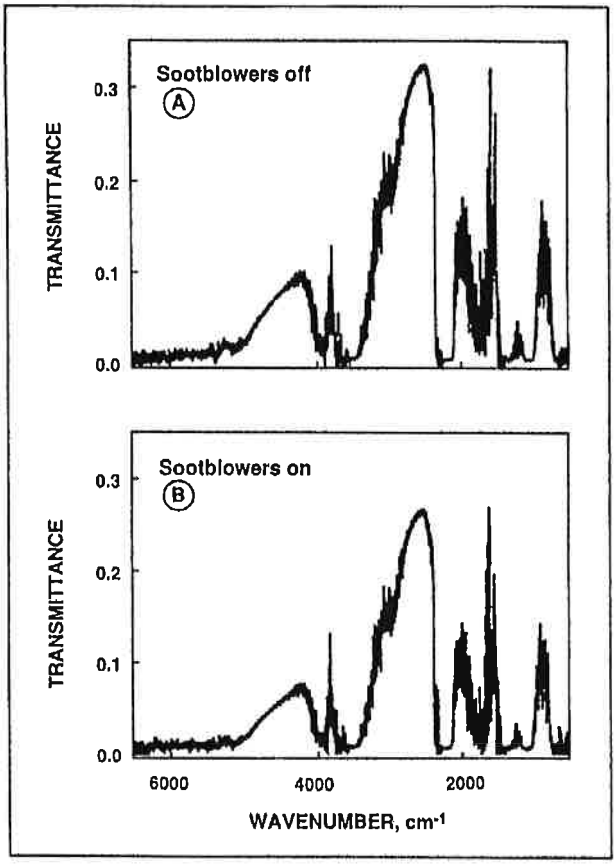

The observed transmittance changes with different operating conditions. **Figure 5** contains transmittance and normalized radiance spectra taken through the boiler at two different flow rates of liquor (200 gal/min and 325 gal/min). The most obvious change is the transmittance through the fume: the higher flow (Fig. 5C) has a substantially reduced transmittance compared to the lower flow rate (Fig. 5B). The normalized radiance also shows that both the gas and wall temperatures increase by 100 K when the flow increases from 200 gal/min to 325 gal/min. Less obvious are the changes in the H_2O and CO_2 levels.

In a similar fashion, **Fig. 6** shows the transmittance spectra of the boiler under the conditions of sootblowing. At most times, the sootblower located below the FTIR measurements is not operating, and one obtains a relatively high transmittance, as shown in Fig. 6A. However, in a separate experiment, we can manually operate the sootblower during scanning to yield the spectrum shown in Fig. 6B. As shown, the amount of blockage due to the fume increases during sootblowing either because the sootblower is generating new particles when cleaning the heat exchanger or because it is mixing a stream more heavily laden with particles into the path of the IR beam. The normalized radiances are not shown because there is no change in the measured temperatures ($T_{gas} = T_{particle} = 1125$ K, and $T_{wall} = 975$ K).

Discussion

Gas analysis

It is possible to quantitatively measure the H_2O and CO_2 concentrations by analyzing the wings of their absorption bands. Since this information is relatively uninteresting for this initial experiment, we have not calculated concentration values for H_2O and CO_2. Far more interesting are the minor species like CO and H_2S, which indicate combustion efficiency and recovery efficiency. Three factors limit the instrument's sensitivity in detecting minor species of gases: noise in the spectra, interferences by the absorption bands of major species (H_2O and CO_2), and particle interferences.

Noise. There are many sources of noise in the boiler measurements that do not normally appear in conventional laboratory measurements. One source is flicker noise arising from the turbulent nature of the sample. Since the gases and particles are hot, any turbulence of the sample stream causes modulated IR radiation to impinge on the detector and produce spurious signals in the interferogram. After Fourier transformation, these spurious signals appear as noise in the spectrum.

Cold moving particles can also cause a similar problem. Called "transit" noise, the moving particles pass in and out of the IR beam and cause a transient modulation of the IR intensity. The detector duly records this modulation as signal, and noise appears in the spectrum.

A lesser source of noise is the lensing of the IR beam by the hot gases. Exactly the same as "heat devils" rising off a hot pavement, time variations in the gas temperature produce changes in the refractive index of the gas that steer the IR beam slightly in and out of focus. Noise is the result.

All of these noise sources combined produce boiler transmission spectra with 5 times more noise than spectra taken outside the boiler (0.5% vs. 0.1% for 1 min of scan time). Fortunately, there are several techniques to reduce noise from these sources.

In most cases, the noise is low in frequency and would appear, after Fourier transformation, primarily as artifacts at low wavenumbers. For the cases in which the primary artifacts appear below 500 cm^{-1}, the effect is completely negligible because the Hg Cd Te detector cuts off at 500 cm^{-1}, and there is no useful spectral information below that point. There are still some secondary effects that are not removed, but the technique of signal averaging spectra reduces them according to the square root of the number of scans.

Interferences by the absorption bands of major species. A more serious threat to sensitivity is the interferences of H_2O, CO_2, and fume. Because these species are so abundant, significant regions of the spectrum are completely blocked and are totally useless. The most damaging of the three is H_2O because it has a number of wide absorption bands. In principle, with enough spectral resolution, one can distinguish between two gases that have bands that overlap. One would then "see" between the water lines. In the data presented here, the resolution is 4 cm^{-1} and is insufficient to resolve the water absorption lines from other gases. The necessary resolution is 0.5–1 cm^{-1} and is available on newer models of the M110 and other rugged FTIR spectrometers.

There is a performance price for the increased resolution, however. For a constant signal-to-noise ratio (SNR), theory shows that $\Delta\nu t^{1/2}$ is a constant, so increasing the resolution from $\Delta\nu$ = 4 cm^{-1} to 1 cm^{-1} requires 16 times as much signal averaging time to achieve the same noise level.

Partially offsetting this time penalty is the fact that the absorbance of weak narrow gas lines is roughly four times larger at 1 cm^{-1} than at 4 cm^{-1} (*10*). As a result, one requires four times as much signal-averaging time to achieve the same sensitivity limit at 1 cm^{-1} as with 4 cm^{-1}. Sixteen times as much signal averaging would decrease the limit by a factor of four. Thus, removing narrow line interferents (like H_2O) increases total measurement time by $\Delta\nu^{-1}$. Please note that for species with broad gas lines (SO_2, NO_2, dimethyl sulfide, etc.), the increased resolution merely increases the required measurement time without improving the sensitivity limit.

Particle interferences. Particles also create problems if $N A F_{ext}$ is so large that $\tau = 0$, and the particles completely block out portions of the spectrum. This problem occurs in a broad spectral region at high wavenumbers because of scattering and also in the fume's absorption band at 1200 cm^{-1}. When this occurs in the transmittance spectrum, there is no recourse. In emission, however, one can still obtain useful information in the scattering region.

Because gases are generally at a higher temperature than the boiler walls, the normalized radiance shows the hot gas bands sitting on top of the wall R_n. Since the radiance contains the same information as the transmission if one knows the temperature (Eq. 2), one can use the normalized radiance to yield concentration. In Fig. 5, for example, the water and CO_2 bands near 5000 cm^{-1} are completely lost in the transmittance spectra but are easily seen in the normalized radiance. Given the gas temperature determined from Fig. 5B and baseline-subtracting the wall's normalized radiance, one sets radiance equal to $(1 - \tau)\, R_b(\nu,T)$ and determines τ.

Table II lists the sensitivity limits for a variety of sulfur and nitrogen compounds plus CO and HCl. In all cases, it is assumed in the calculations that the pathlength is 11 m, that the absorption signal is three times the noise level, that HgCdTe detectors are being used, and that temperature and pressure are at standard values. (One must correct the data for temperatures other than 273 K.)

The column on the left represents the best case scenario, while the column on the right represents true operating conditions. The first column is the predicted sensitivity at 1 cm^{-1} resolution using an assumed noise level of 0.1% of the signal level. This is the noise level we have observed in the *ex-situ* reference after scanning for 1 min at 4 cm^{-1}. The scanning time at 1 cm^{-1} would be 16 min.

For the first column, we assume there are no interferents like water or fume. Please note that most of the sensitivity levels are less than 1 ppm except for H_2S, which does not absorb strongly. The second column shows the sensitivity levels expected in the boiler itself, assuming a resolution of 1 cm^{-1} and a noise level of 0.5%. The higher noise level accounts for the observed noise in a spectrum taken through the boiler. The higher noise raises the sensitivity limit by a factor of five. The middle column represents the levels for the same noise level (0.5%) but at 4 cm^{-1}. Despite the large reduction in scan time, many of the sensitivity limits are unaffected by degrading the resolution to 4 cm^{-1} because those gases have relatively broad absorption lines. For the narrow line gases like H_2S, CO, NO, and HCl, the limit increases by a factor of four.

Up to this point, we have not considered the effect of interferents. Factoring in a typical amount of H_2O into the spectrum (3%), one finds that most of the sensitivity levels are unchanged except for those of SO_2 and CS_2. In the case of the CS_2, the water band completely blocks all radiation within the CS_2 band. Adding fume to the spectrum (Column 5) completely blocks the SO_2 band. Nevertheless, the sensitivity levels remain below 10 ppm except for NO (approx. 300 ppm) and the blocked gases (SO_2 and CS_2). Note that the CO level in this boiler is commonly 10–100 ppm. Since none of these gases are observed, they must exist at levels below those shown in Table II.

Particle analysis

Using the $k(\nu)$ and $n(\nu)$ spectra for fume, one can calculate the extinction coefficient Q_{ext} using Eq. 4 and can predict a transmittance based on Eq. 1. **Figure 7** shows Q_{ext} based on three different particle sizes—0.2 μm, 0.4 μm, and 0.6 μm. in diameter. As expected, larger particles have a higher extinction than smaller particles because both the scattering and absorption increase. Note, however, the relative heights of the scattering effect and the absorption peak change with particle size. Using such spectra, we now fit Q_{ext} of various sizes to an absorption spectrum to yield the size and number density of the fume.

By rearranging Eq. 1, we see that the absorbance (which is equal to -log [τ]) is proportional to $[k_i(\nu)C_i + N A F_{ext}(\nu)]L$. **Figure 8** shows the absorbance spectrum calculated from Fig. 4A. Keep in mind that the noise in Fig. 4A equals 0.005, so any absorbance feature in Fig. 8 above -log[0.005] = 2.3 is noise and may not be a true absorbance feature.

By assuming $Q_{ext} = F_{ext}$, one can multiply the spectra of Fig. 7 by the factor $N A L$ until they fit the sloping baseline of the absorbance spectrum. To do this, we use the parts of the spectrum between 4800–4300 and 2700–2500 cm^{-1}. Fits using the three different particle sizes appear in Fig. 8. None of the spectra from Fig. 7 can adequately fit the sloping baseline without an arbitrarily chosen baseline offset. Ignoring for the moment the need to explain the offset, one finds that the 0.2-μm particle size is incorrect because the fume absorption features are too large to be consistent with the observed absorbance spectrum. (Note the shoulders of the absorption peak in Fig. 8A.) Similarly, the 0.6-μm particle size is also incorrect since it predicts absorption peaks that are too small to fit the measured spectrum (Fig. 8C).

The best fit is clearly the 0.4-μm particle size, which is consistent with the size used in the KBr pellet analysis (0.35 μm). One can then convert the fitting constant NAL into a number density that corresponds to $4.8 \times 10^7/cm^3$ [where L = 11 m and $A = 1/4\pi\ (0.4\ \mu m)^2$]. This number density falls in the expected range as determined by a mass balance based on the recycle rate. The values of N for other operating conditions are $N_{200\ gal/min} = 4.7 \times 10^7/cm^3$ and $N_{blowers\ on} = 5.5 \times 10^7/cm^3$.

Looking back on the spectra of Figs. 5 and 6, one may be surprised by the small change in N compared to the large changes in $\tau(\nu)$. The explanation for this is that the

7. Predicted extinction efficiencies of fume based on the optical constants of Fig. 3B and C.

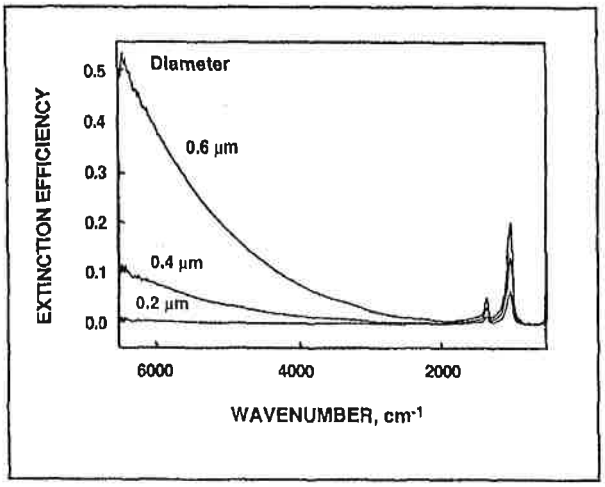

8. Comparisons of predicted extinction spectra of fume to measured absorbance spectrs, using Q_{ext} for fume of particles 0.2 μm, 0.4 μm, and 0.6-μm in diameter

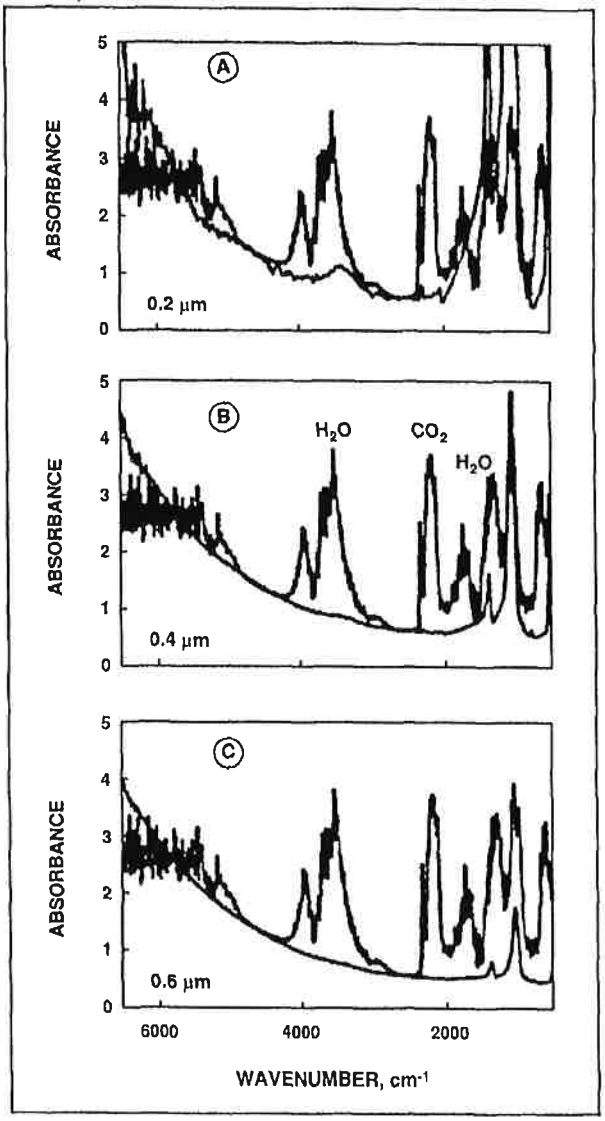

offset changes from spectrum to spectrum, with most of the change in τ occurring in the change in the offset. The offset for 200 gal/min is 0.24 absorbance units (au), 0.45 au for 325 gal/min, and 0.51 au for 325 gal/min with the sootblowers on.

Baseline offset and errors in the *ex-situ* reference

Noting that the baseline offset must be independent of wavenumber, one is left with three possible explanations. Large particles like carry-over could cause the baseline shift observed since the Q_{ext} for them is approximately constant throughout the IR path as long as their diameters are > 75 μm. One can test the plausibility of this argument by estimating the extinction due to carry-over particles using an observed number density of about 2/cm^3 and a typical size of 75 μm. Noting that large-diameter particles have $F_{ext} \sim 1$ and substituting into $N\ A\ F_{ext}L/2.303$, one obtains approximately 0.05 au. Thus, some of the offset may be due to carry-over particles, but probably not all of it is.

A second possible explanation for the offset is detector saturation. HgCdTe detectors respond nonlinearly if the amount of IR radiation is too high. This situation can occur when measuring the transmittance of a hot sample or flame and causes the baseline to shift to lower values; absorption features are not greatly affected. Consequently, the absorbance spectrum appears to be shifted to higher values by a constant. The magnitude of this shift is relatively small, typically corresponding to less than 0.2 au ($\tau = 0.63$). Once again, this explanation can account for some of the offset but not all. If it is a problem, future experiments can be carried out using nonsaturating HgCdTe detectors developed in our laboratory.

The third possible explanation for the offset is the most likely: an error in the *ex-situ* reference. Any difference in the alignment of the optics between the boiler measurements and the *ex-situ* reference would produce a baseline shift in the spectrum. As mentioned, several different measurements of the *ex-situ* reference verify the reproducibility of the method for aligning the optical system but not its accuracy.

Such an alignment error is not disastrous, however. For gases, this problem has no effect on the accuracy of the measured gas absorption: any baseline offset disappears during the baseline correction to remove the particle extinction. Temperature measurements are also not affected because, within the strong absorption bands of the H_2O, CO_2, and fume, the transmittance spectrum is zero and the normalized radiance equals the radiance. A similar argument holds for the wall temperature measurement since the transmittance of the fume at high wavenumbers is also zero.

The biggest problem arises when determining the particle concentration because the number density depends on having an absorbance baseline of zero. If the particles are not large and have unique absorption bands (e.g., fume), one can use Mie theory to predict F_{ext} and then fit F_{ext} to the measured spectrum, assuming an arbitrary

baseline offset. The quality of the fit relies on matching the scattering tail at high wavenumbers and on matching the shoulders of the absorption bands. If there are no unique absorption bands (e.g., submicron soot or large particles), then one cannot conclusively fit the size and number density. In such a case, the projected area of the particles can be determined as long as the reference is accurate. At this time, we cannot conclude how much of the observed offset is due to large particle blockage.

Conclusions

The results show that the E/T FTIR can function in the harsh environment of the recovery boiler and provide useful information. The entire procedure of assembly, data collection, and disassembly has required less than five days, and it takes place without interrupting or modifying boiler operation. The FTIR spectra yield information on the gases (concentration and temperature), particles (size, concentration, and temperature), and walls of the boiler (temperature).

At 4 cm^{-1} resolution and 1 min of scan time, the only observed gases are CO_2 and H_2O. Other gases are below the detection limits described in Table II. (Multiply by ~ 4 to correct for temperature-induced changes in concentration.) Temperatures of the gases range from 1025 K (liquor = 200 gal/min) to 1125 K (liquor = 325 gal/min); sootblowing has no effect on temperature.

The FTIR spectra also show that the fume cloud is reasonably transparent to mid-range IR radiation. After measuring the optical constants of fume in the laboratory, one can then use Mie theory to predict fume extinction and fit that value to the observed absorbance spectra. Such fits indicate that the fume has a diameter of about 0.4 μm and that its number density in the boiler is roughly 4.8 $\times 10^7/cm^3$ during both low-flow and high-flow conditions; the number density rises about 15% during sootblowing upstream. The temperature of the fume matches the gas temperature, and the wall temperature is consistently 150 K below the gas temperature. Some information on the spatial distribution of the fume temperature and the wall temperature is also present in the radiance spectra.

There are several issues that require further attention. Lowering the sensitivity limits in Table II is highly desirable. By scanning 16 min at 1 cm^{-1} and 4 cm^{-1} resolutions, one can decrease the limits by a factor of 4 or more. Performing measurements after the precipitator would also aid the analysis of SO_2 and CS_2. A second problem is the unexplained baseline offset when fitting the fume spectra. The offset is due either to large particles like carry-over, to detector saturation, or to an error in the optical alignment. This problem does not affect gas or temperature measurement, but it does leave the amount of large particles somewhat in doubt. Resolving this issue will require using a nonsaturating detector and temporarily shutting off the liquor flow to acquire an *in-situ* reference and then comparing the *in-situ* and *ex-situ* references.□

Literature cited

1. Adams, T. M. and Frederick, W. J., Kraft Recovery Boiler Physical and Chemical Processes, American Paper Institute, New York, 1988.
2. Best, P. E., Carangelo, R. M., Markham, J. R., and Solomon, P. R., Combustion and Flame 66: 47(1986).
3. Solomon, P. R., Best, P. E., Carangelo, R. M., Markham, J. R., *et al.*, proceedings, 21st Symposium (International) on Combustion, The Combustion Institute, Pittsburgh, 1986, p. 1763.
4. Solomon, P. R., Chien, P. L., Carangelo, R. M., Best, P. E., *et al.*, proceedings, 22nd Symposium (International) on Combustion, The Combustion Institute, Pittsburgh, 1988, p. 211.
5. Best, P. E., Chien, P. L., Carangelo, R. M., and Solomon, P. R., Combustion and Flame 85: 309(1991)
6. Markham, J. R., Zhang, Y. P., Carangelo, R. M., and Solomon, P. R., 23rd Symposium (International) on Combustion, The Combustion Institute, Orleans, France, 1990, p. 1869.
7. Bohren, C. F. and Huffman, D. R., Absorption and Scattering of Light by Small Particles, Wiley, New York, 1983, p. 135.
8. Solomon, P. R., Carangelo, R. M., Best, P. E., Markham, J. R., *et al.*, 21st Symposium (International) on Combustion, The Combustion Institute, Pittsburgh, 1986, p. 437.
9. Solomon, P. R., Carangelo, R. M., Best, P. E., Markham, J. R., *et al.*, Fuel 66: 897(1987).
10. Griffiths, P. R. and de Haseth, J. A., Fourier Transform Infrared Spectrometry, Wiley, New York, 1986, p. 255.

Received for review May 6, 1991.
Accepted July 31, 1991.

CORRECTION

Keynote speaker incorrectly quoted

In the Conference Report, "International mechanical pulping trends" published in the September issue (p. 254), Douglas Atack, the keynote speaker of the International Mechanical Pulping Conference, was misquoted.

In the report Atack was quoted as follows: "ONP could replace 10,000 tons of mechanical pulp in newsprint annually."

The correct quote is: "By the end of the decade increased use of recycled fiber could displace as much as 10 million tones a year of virgin mechanical pulp from newsprint furnishes throughout the world."